Available online at www.sciencedirect.com
SCIENCE DIRECT®
Journal of Power Sources 145 (2005) 563–571
JOURNAL OF POWER SOURCES
www.elsevier.com/locate/jpowsour

Three-dimensional modeling and experimental investigation for an air-breathing polymer electrolyte membrane fuel cell (PEMFC)

Wang Ying [a,b], Young-Jun Sohn [b], Won-Yong Lee [b,*], J. Ke [a], Chang-Soo Kim [b]

[a] *Mechanical Engineering School, Southwest Jiaotong University, Chengdu, 610031 Sichuan, PR China*
[b] *Fuel Cell Research Center, Korea Institute of Energy Research, P.O. Box 103, Yusong, Daejeon 305-343, South Korea*

Accepted 6 January 2005
Available online 26 April 2005

Abstract

An air-breathing polymer electrolyte membrane fuel cell bears many advantages, which are important for portable-power applications. However, several barriers must be overcome before an air-breathing PEMFC achieve commercially wide-scale adoption. In this paper, with emphasis on improving the performance of air-breathing PEMFC, the simulation and experiment has been done simultaneously. Considering the natural convection in the cathode side, electrochemical reaction in the catalyst layer, water transport in the membrane, a coupled three-dimensional complex model has been developed in this work. The parameters which greatly affect the performance of an air-breathing PEMFC have been calculated for the base case such as the distribution of water and reactant, temperature and electrochemical performance. To validate the numerical result, the experiment test system have been designed to investigate the temperature distribution and cell performance. The results from this work show that the performance of air-breathing PEMFCs is strongly affected by natural convection feature. The concentration losses play a major role on the cell performance. The ambient relative humidity also has significant effect on the cell performance. The fields of water, temperature, velocity and electrochemical reaction have strong interaction on each others.

Keywords: Air-breathing PEMFC; Natural convection; Humidity; Mass transport limitation

1. Introduction

Small fuel cells have provided significant advantages in portable electronic applications over conventional battery systems. However, the typical polymer electrolyte fuel cell system with its heavy reliance on subsystems for cooling, humidification and air supply would not be practical in small applications. The air-breathing polymer exchange membrane fuel cells (PEMFCs) without moving parts (external humidification instrument, fans or pumps) are one of the most competitive candidates for future portable-power applications. An air-breathing PEMFC design in our laboratory is illustrated in Fig. 1. When this cell is working, the heat generated due to irreversibility of fuel cell. Meanwhile, the oxygen is consumed and water is produced in catalyst layer. The gas mixture density is accordingly changed based on ideal gas's law. The heated fluid becomes less dense and flows upwards, while packets of cooled fluid become denser and sink because of buoyancy force. Therefore, the air in the ambient is induced into cathode channel like a breath and the cathode reactant is replenished. The convection caused by temperature difference or concentration gradient is called natural convection or free convection. The PEMFCs in which the air is breathed into cell by natural convection is so called air-breathing PEMFCs. However, there are several problems should be envisaged to attain a commercially viable portable-power generation system for air-breathing PEMFCs. In the natural convection, the velocity profile depends on temperature and concentration gradient which affected by electrochemical reaction and material properties. When the air flow rate in the cathode channel is insufficient due to weak natural convection or the liquid water exists in cathode channel and diffusion layer so that the gas way for oxygen transport is blocked when cell

* Corresponding author. Tel.: +82 42 860 3506; fax: +82 42 860 3739.
E-mail address: wy82lee@kier.re.kr (W.-Y. Lee).

0378-7753/$ – see front matter © 2005 Elsevier B.V. All rights reserved.
doi:10.1016/j.jpowsour.2005.01.083

Nomenclature

A_{cv}	specific area for control volume ($m^2\ m^{-3}$)
B	coefficient in concentration over potential equation
C_p	specific heat capacity at constant pressure ($J\ K^{-1}\ kg^{-1}$)
D_w	effective diffusion coefficient of water in the membrane
F	Faraday's constant, 96,487 C/equivalent
g	gravity ($m\ s^{-2}$)
h_m	mass transfer coefficient ($m\ s^{-1}$)
I	local current density ($A\ cm^{-2}$)
I_{lim}	concentration limiting current density ($A\ cm^{-2}$)
I^0	exchange current density ($A\ cm^{-2}$)
k_{eff}	effective thermal conductivity
k_p	hydraulic permeability (cm^2)
L	characteristic length (m)
m	mass fraction
M	molar mass of gases ($kg\ mol^{-1}$)
n_d	electro-osmotic drag coefficient
R	gas constant, 8.314 $J\ mol^{-1}\ K^{-1}$
S	source term in governing equation
Sh	Sherwood number
t_m	membrane thickness (mm)
T	temperature (K)
$\breve{u}$	velocity ($m\ s^{-1}$)
V	voltage (V)
V_{oc}	open circuit voltage (V)
x, y, z	Cartesian coordinates

Greek letters

α	net water transfer coefficient per proton
∇	change in ...
ε	porosity
η	over potential (V)
μ	dynamic viscosity ($kg\ m^{-3}$)
ρ	density ($kg\ m^{-3}$)

Superscripts and subscripts

a	anode
act	activation
b	ambient
c	cathode
conc	concentration
H_2	hydrogen
H_2O	water
ohm	Ohmic losses
O_2	oxygen
u	momentum source
v	vapor
w	water

working at high ambient humidity, the oxygen consumed in catalyst layer could not be replenished. Thus the performance of air-breathing PEMFCs could be greatly diminished due to concentration losses. From previous research it is proved that the concentration losses due to oxygen transport limitation are much higher than typical forced convection PEMFCs [1–6]. Water management is another problem which greatly affects performance of air-breathing PEMFCs. When the air-breathing PEMFC works at low humidity, because the all water source is only from the water product in cathode reaction and air humidity, the membrane is easy to be dehydrated in anode side. And then the proton transfer resistance strongly increases because of low protonic conductivity of membrane. Reversely, when air-breathing working at high ambient humidity, the vapor water condensed into liquid and then blocks the gas way resulting in serious oxygen transport limitation. To further the development and improvement of the air-breathing PEMFCs, understanding the phenomena inside cell through the experiment and numerical calculation is apparently significant.

In previous studies, many pioneers have contributed to the modeling of fuel cells. Most early studying is one-dimensional (1D) or two-dimensional (2D) flows [7–13]. Undoubtedly, those works have provided useful insight and fundamental understanding, but primarily analytic and required a number of simplifications. The full solution for fluid dynamics and thermodynamics equations could not be included in those models due to limitation of numerical techniques. To predict the performance of fuel cells, investigate the operation of fuel cells and optimize the distribution of gas, recently some 3D models have developed and solved in different extent of complexity including single or two-phase modeling [23,24] in several papers using the methods of computational fluid dynamics [14–19]. However, surveying available literatures, few Papers addressed to modeling of the air-breathing PEMFC. Schmitz [20] developed a two-dimensional isothermal model, and discussed the different channel opening ratio's effect on the fuel cell's performance. Li et al. [21] studied mass transfer in a free convection PEMFC using theoretical analysis being analogy with heat transfer and experiment testing to investigation the effect of mass transfer on cell performance.

The objective of this paper of this study is to develop a three-dimensional model to account for the effect of flow dynamic, heat/mass transport and electrode kinetics on the performance of an air-breathing PEMFC. The model is validated via single cell experiment testing performed in fuel cell center of KIER.

2. Mathematic models

Modeling of an air-breathing PEMFC is challenging, because the processes involve many coupled physical phenomena such as multi-component, multi-dimensional flow, heat and mass transfer with electrochemical reactions,

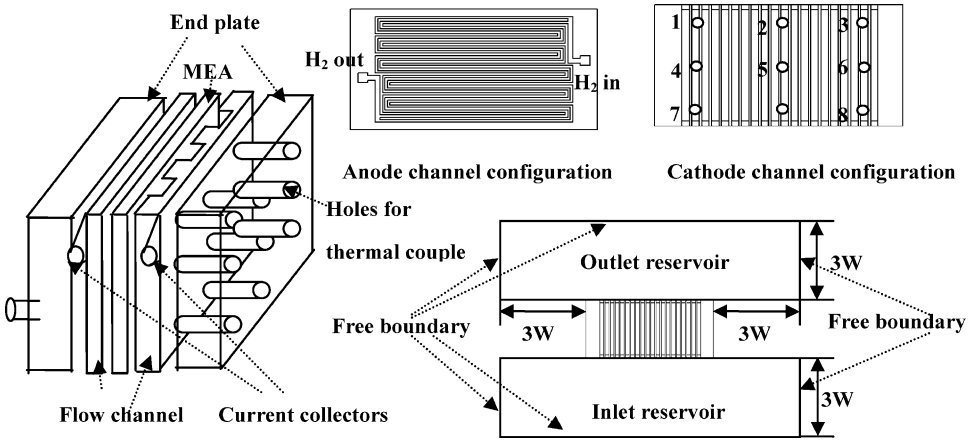

Fig. 1. Geometry of an air-breathing PEMFC.

natural convection in cathode, conjugate heat transfer between fluid and solid, and transport in porous medium. A better understanding of these transport processes will provide efficient water management, alleviate mass transport limitation, and improve cell performance. All equations included in this model are presented below.

2.1. Governing equations

In the gas flow field, the flow is laminar steady state flow. The governing equations of fluid flow represent mathematical statements of the conservation laws of physics. Considering special coupled electrochemistry here, all governing equation and source term is summarized in Table 1.

The momentum equation and energy equation are coupled via equation of state of ideal mixtures.

$$\rho = \frac{P}{RT\left(\sum X_{\mathrm{m}}/M_{\mathrm{m}}\right)} \tag{1}$$

In governing equation, ε is porosity for porous medium. It is 0.4 for diffusion layer, 0.28 for catalyst layer, and 1.0 for other region.

2.2. Water transport in membrane

Water exists in the form of vapor when the air-breathing PEMFCs working in low ambient humidity. Two mechanisms for vapor water transport from anode to cathode in the fuel cells is considered: (i) electro-osmotic drag, which is cause by proton transport from anode side to cathode side of the membrane; (ii) back-diffusion, which is due to the concentration gradient of water created by water generation in cathode reaction.

To minimize the complexity of model it is assumed that the gradient of water concentration across the membrane can be approximated by a single-step linear difference between the concentration in cathode and in anode because the membrane in this studying is enough thin. The final expression net water molecular per proton flux can be yielded as:

$$\alpha = \frac{n_{\mathrm{d}} - FD_{\mathrm{w}}(C_{\mathrm{w,c}} - C_{\mathrm{w,a}})}{It_{\mathrm{m}}} \tag{2}$$

Here the diffusion coefficient, electro-osmotic coefficient depends on water content in membrane that is decided by water activity. The detailed equations have already developed by Springer et al. [9].

2.3. Electrochemical equations

In this model activity over-potential in catalyst layer, ohmic resistance in membrane and oxygen transport limited over-potential in cathode reaction layer are involved in voltage losses. The detailed equation is described as

Table 1
Summary of governing equations in MEA

	Conversation equation	Source term			
		GDL	Anode catalyst layer	Cathode catalyst layer	MEM
Mass	$\nabla\cdot(\varepsilon\rho u^{\boldsymbol{\varpi}}) = S_{\mathrm{m}}$	0	$S_{\mathrm{H_2}} + S^{\mathrm{a}}_{\mathrm{H_2O}}$	$S_{\mathrm{O_2}} + S^{\mathrm{c}}_{\mathrm{H_2O}}$	0
Momentum	$\nabla\cdot(\rho u u^{\boldsymbol{\varpi}\boldsymbol{\varpi}}) = -\nabla P + \nabla\cdot(\mu\nabla u^{\boldsymbol{\varpi}}) + S_{\mathrm{u}}$	$-\frac{\mu u^{\boldsymbol{\varpi}}}{k_{\mathrm{p}}}$	$-\frac{\mu u^{\boldsymbol{\varpi}}}{k_{\mathrm{p}}}$	$-\frac{\mu u^{\boldsymbol{\varpi}}}{k_{\mathrm{p}}}$	0
H_2	$\nabla\cdot(\varepsilon\rho m_{\mathrm{H_2}} u^{\boldsymbol{\varpi}}) = \nabla\cdot(D^{\mathrm{eff}}_{\mathrm{H_2}}\nabla\rho m_{\mathrm{H_2}}) + S_{\mathrm{H_2}}$	0	$-\frac{IM_{\mathrm{H_2O}}A_{\mathrm{cv}}}{2F}$	0	0
O_2	$\nabla\cdot(\varepsilon\rho m_{\mathrm{O_2}} u^{\boldsymbol{\varpi}}) = \nabla\cdot(D^{\mathrm{eff}}_{\mathrm{O_2}}\nabla\rho m_{\mathrm{O_2}}) + S_{\mathrm{O_2}}$	0	0	$-\frac{IM_{\mathrm{O_2}}A_{\mathrm{cv}}}{4F}$	0
H_2O	$\nabla\cdot(\varepsilon\rho m_{\mathrm{H_2O}} u^{\boldsymbol{\varpi}}) = \nabla\cdot(D^{\mathrm{eff}}_{\mathrm{H_2O}}\nabla\rho m_{\mathrm{O_2}}) + S_{\mathrm{O_2}}$	0	$S^{a}_{w} = -M_w A_{cv}\alpha I/F$	$S^{c}_{M} = -IM_{\mathrm{O_2}}A_{cv}/4F + IM_w A_{cv}/2F + \alpha IM_w A_{cv}/F$	0
Energy	$\nabla\cdot(\varepsilon\rho c_{\mathrm{P}} u^{\boldsymbol{\varpi}} T) = \nabla\cdot(k^{\mathrm{eff}}\nabla T) + S_{\mathrm{T}}$	0	$I\eta_{\mathrm{a}}$	$I\eta_{\mathrm{c}}$	$I\eta_{\mathrm{m}}$

Table 2
Values for parameters and boundary condition used in the model

Parameters	Symbol	Value	Parameters	Symbol	Value
Porosity in carbon paper and catalyst layer	ε	0.4, 0.28	Cathode channel height and width	h_c, w_c	0.3 cm
Average current density	I_{avg}	0.15 A cm^{-2}	Relative humidity in air	ξ	63% RH
Ambient temperature, pressure	T_b, P	299 K, 101325 Pa	Membrane dry density	ρ_{dry}	1840 kg m^{-3}
Anode channel width, height	w_a, h_a	0.1 cm	Membrane dry equivalent weigh	M_{dry}	1100 kg kmol^{-1}
H_2 inlet temperature	T_a	299 K	Membrane thickness	t_m	0.00508 cm
H_2 flow rate in inlet	N_{H_2}	7.198E−08 kg s^{-1}	Thickness of diffusion layer, catalyst layer	t_d, t_s	0.026 cm, 0.001 cm
Permeability in GDL	k_p	1.8E−18 m^2	Oxygen/nitrogen ratio in air	ζ	0.21/0.79
Permeability in catalyst layer	k_p	1.76E−12 m^2	Cathode channel length	L_c	47 mm

following:

$$V_C = V_{OC} - \eta_{act} - \eta_{ohm} - \eta_{conc} \tag{3}$$

$$\eta_{act} = \frac{RT}{0.5F \ln(I/I^0 P_{O_2})} \tag{4}$$

$$\eta_{ohm} = \frac{t_m I}{\sigma_m} \tag{5}$$

$$\eta_{conc} = BT \ln\left(1 - \frac{I}{I_{lim}}\right) \tag{6}$$

The dimensionless oxygen mass transfer coefficient Sherwood number is calculated by:

$$Sh = \frac{h_m^{O_2} L}{D_{O_2}} \tag{7}$$

At the limiting current density an electrochemical system is under mass transport control. A surface concentration of zero corresponds to the limiting current density condition, and then the limited current density equation becomes [22]:

$$I_L = \frac{4FD_{O_2} c_{O_2}^{\infty} Sh}{L} \tag{8}$$

2.4. Boundary and initial conditions

The numerical domain used here include full single cell geometry region. In the cathode side, air is induced into cathode channel from bottom opening and discharged from the top vent by natural convection. It is evident the velocity and pressure values at the inlet and exit sections are not known a priori. Hence computation domain was extended well beyond the geometrical configuration to free boundary condition where the pressure must be equal to that of the undisturbed environment. The computation domain except the real physical domain is called reservoirs. The minimum vertical and horizontal size of reservoirs has been estimated as shown in Fig. 1. The hydrogen flow rate in the inlet was calculated based on average current density and hydrogen stoichiometric. Other detailed boundary condition used in the model can be found in Table 2.

2.5. Solution algorithm

The governing equations and appropriate boundary conditions were implemented and solved in commercial Computational Fluid Dynamics software STAR-CD V3.15A that employs a finite volume formulation. All processes were operated in LINUX. MARS (monotone advection and reconstruction scheme) and SIMPLE algorithm was used to solve the governing equations. The governing equations for electrochemical reaction in the MEA and water transport in membrane were simultaneously solved by user subroutine in form of FORTRAN code based on finite differential approach. The source terms for mass and energy conservation equations were calculated by a given value of average current density and estimated over-potential at the first. And then the mole fraction, temperature, and other parameters in fluid field were obtained from the solution in STAR-CD, which were used to calculate the local current density, over-potential and net water transport molecular in membrane for next iteration. Then the source terms were upgraded using these calculated local current density and over-potential. These processes were iterated until the residuals agree with the specified values.

3. Experimental

The aim of this experiment study is to demonstrate numerical calculation for an air-breathing PEMFC. The performance of the fuel cell was characterized with polarization and current transient measurements. Because the temperature is vital parameters for natural convection, the temperature in the anode plate and cathode carbon paper surface were also tested.

3.1. Experiment preparation

Fig. 1 shows the schematic of the air-breathing PEMFC and temperature test position, the structure of the single cell includes end-plates, gas flow distributor, current collectors, membrane electrode assembly (MEA). The gas distribution plate is made of stainless steel. The material of anode and cathode end plate is aluminum. The gas distribution plates play a role as a current collector and flow field plate for oxygen and hydrogen. The thickness of end plate is relative thick to enable the measurement of cell performance and temperature. For the single cell testing, the small thickness

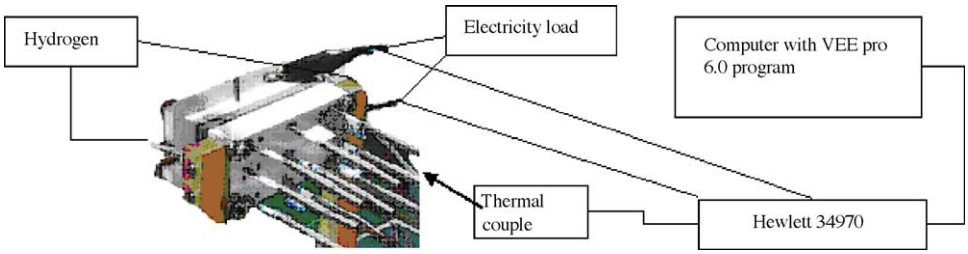

Fig. 2. The schematic test system for an air-breathing PEMFC.

of end plate results in great internal resistance between MEA and plate. Thus the performance of cell strongly decreased due to this contact resistance. The thickness of endplate is 15 mm, and internal resistance of 47 mΩ was demonstrated through testing after preferable assembling. The temperature was measured with a temperature thermal couple located in a hole drilled into the end plate and gas flow plate of cathode side. The 34 cm^2 active area MEA consisted of a Nafion 112 and two electrodes, each comprising a catalyst layer and a gas diffusion layer. The catalyst layer contains dispersed platinum with a loading of 0.3 mg cm^{-2}. The gas diffusion layer is carbon paper. The gas flow channel in cathode is composed of 23 uniformly straight parallel channels with width and thickness of 0.3 cm. Anode flow channel designed in serpentine as Fig. 1 with square area of 0.1 cm × 0.1 cm.

3.2. Measurement procedure

All experiments were carried out in a fuel cell test facility Hewlett Packard 34970A Data Acquisition/Switch unit made by HP corp., which is designed to be mated with the 1 kW electronic loads and HP VEE pro 6.0 program. A laptop was used to control the test station and to record the measurement data through VEE pro 6.0 software. Dry hydrogen was fed to the anode. The stoichiometry of 1 is used for hydrogen flow rate. The air-supply to the cathode was spontaneously obtained by natural convection from environmental air. To test the distribution of temperature, the T type thermal couples were positioned to contact the cathode diffusion layer, the endplate and cathode plate were machined eight holes to insert the thermal couple, the position are illustrated in Fig. 1. The experiment test system is illustrated in Fig. 2.

4. Results and discussions

4.1. Experiment results

The results from the performance measurements are presented in Fig. 3. Effects of ambient humidity can be observed from the curves of voltage and power versus current density, when the ambient humidity is low at 53%, the performance is low due to low humidity in membrane at low current density, but improved when the current load increases and membrane is well hydrated. In this case the liquid water never observed in the channel when the experiment is doing. Therefore, there is not liquid water block in the channel and back diffusion layer. From the results it can be seen that the cell operated at 53% RH has better performance in the mass limitation region (high current density). In this case, the oxygen transport limitation mainly caused by weak natural convection but not liquid water blocking. The performance for low current load is improved when the ambient air humidity increases. When the relative humidity of air is 63%, the performance is better than 53% RH at low current load, but then it is decreased due to liquid water effect. The most liquid water exists in diffusion layer and blocks the gas way from channel to arrive to reaction layer. However, when the air humidity rises up to 77%, the liquid water can be observed in the cathode channel and diffusion layer surface. The liquid water exists in the form of small dew at first, and then it grows up to big dew blocking the gas way, at this time it can be seen that the performance suddenly decreases. Fortunately, only short time latter the water become a water film and then drop down due to gravity forces because the cell arranged in vertical position, while the performance sharply rises up. Therefore, in the case of high air humidity, liquid water also plays a great role in oxygen transport limitation. As a result that the transient performance of cell is really unstable when operated at high humidity. These phenomena can be proved from transient test results of the voltage and current in Fig. 4. In the region marked in a circle when time start from to 300 min, it can be seen that the voltage suddenly decreases and then

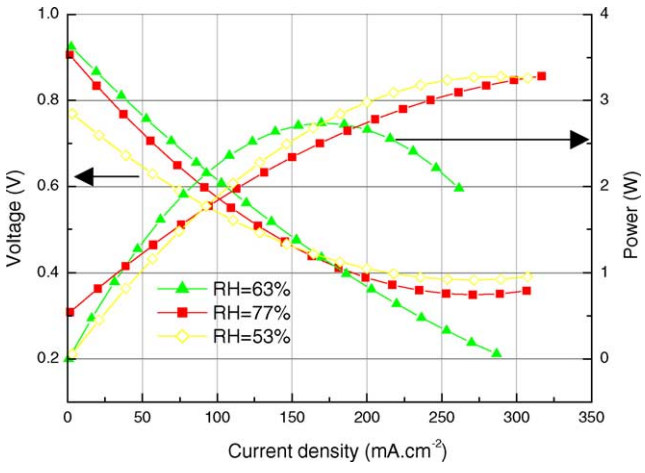

Fig. 3. Cell performance for different operation conditions.

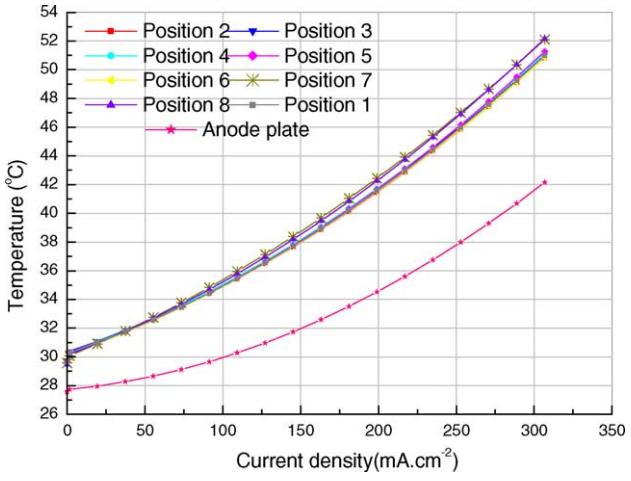

Fig. 4. Transient voltage and current vs. time when ambient humidity is 77%.

increase latter due to liquid water effect. But these phenomena are never found in the case of ambient humidity of 63% (Fig. 5). Another reason to explain that the high performance can be obtained by operated at high humidity is temperature effect that can be found in Fig. 6 and Fig. 7. Comparing these two, the higher temperature was found for 77% RH at same current load because condensation of vapor water releases much heat. The temperature difference is the driven force for natural convection. Therefore the natural convection is enforced, and thus performance is improved. However, it is extremely unstable at high humidity.

For the case of temperature test, it can be seen from Figs. 6 and 7 that the highest temperature can be found in the bottom of side channels, position 7, and 8. This can be explained from the polarization and current density distribution. In these places near the intake of cathode channel, the chemical reaction should be stronger than other regions because enough oxygen supply. And in the side which is near the anode inlet and outlet, the hydrogen is rich in the inlet re-

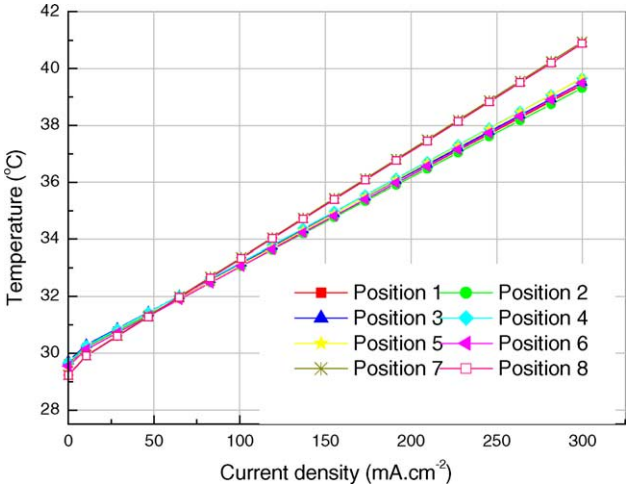

Fig. 5. Transient voltage and current vs. time when ambient humidity is 63%.

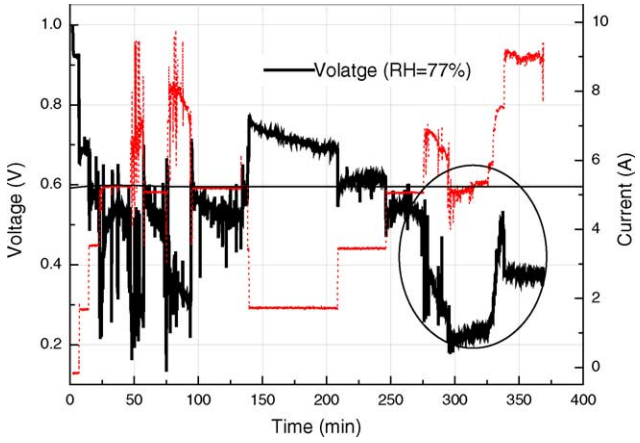

Fig. 6. Temperature profile tested from diffusion layer when humidity is 77%, ambient temperature is 26 °C (°C).

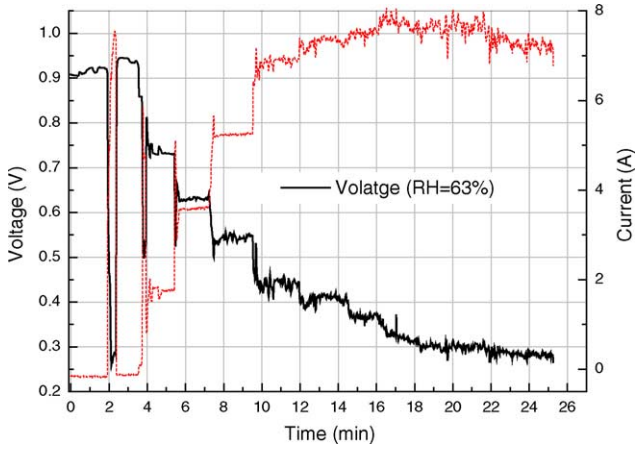

Fig. 7. Temperature profile tested from diffusion layer when humidity is 63%, and the ambient temperature is 26 °C (°C).

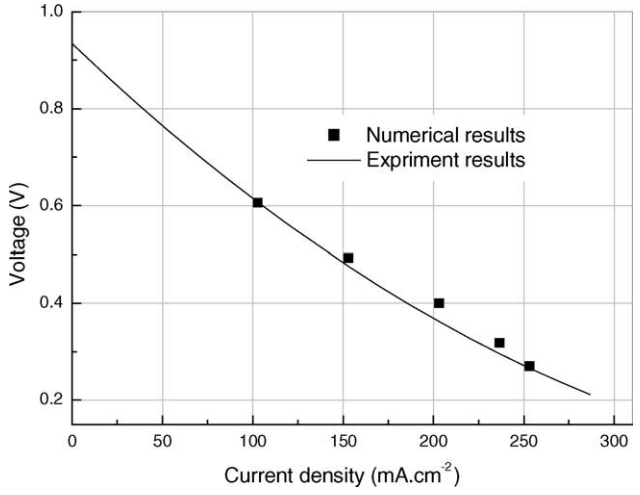

Fig. 8. Comparison between the numerical prediction and experimental results.

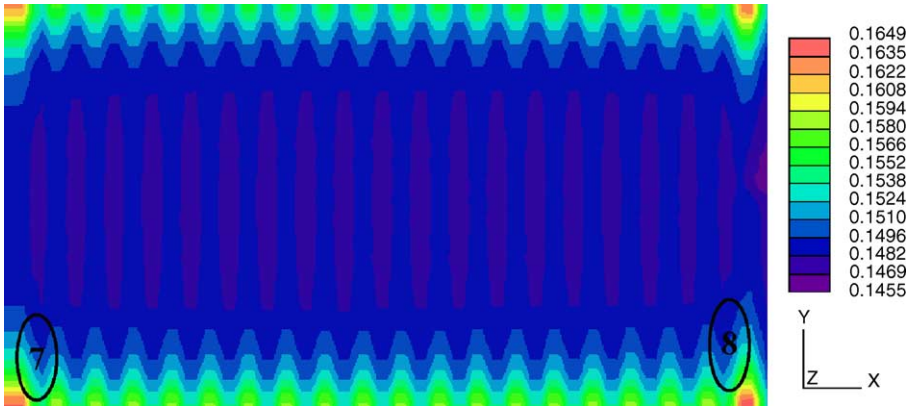

Fig. 9. Current density distribution in catalyst layer surface.

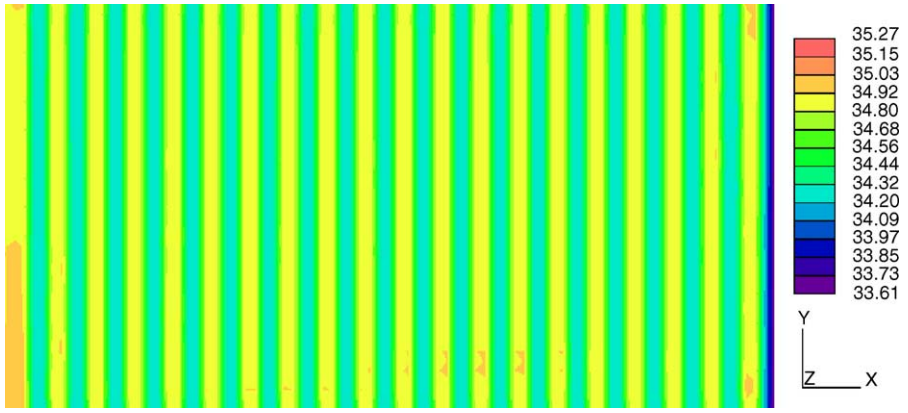

Fig. 10. Temperature distribution in the surface of carbon paper in the side of contacting with cathode gas channel (°C).

gion, and membrane is well hydrated near the outlet region. Hence the electrochemical reaction is strongest.

4.2. Calculation results

The fuel cell terminal voltage is calculated for series of cell current density based the above model and boundary condition in Table 2. Fig. 8 shows the comparison of the relationship between cell voltage and current density from this numerical model with experiment results The black line in Fig. 8 represents the experimental data, square symbols are predicted results. It shows the numerical results agree well with experiment. Some difference between them is because in the experiment the performance is affected by the ambient air condition strongly, and the air condition is not easy to be controlled. Hence the air condition when the experiment was doing is a little different from the calculation operation condition, which is also as a result from electric resistance

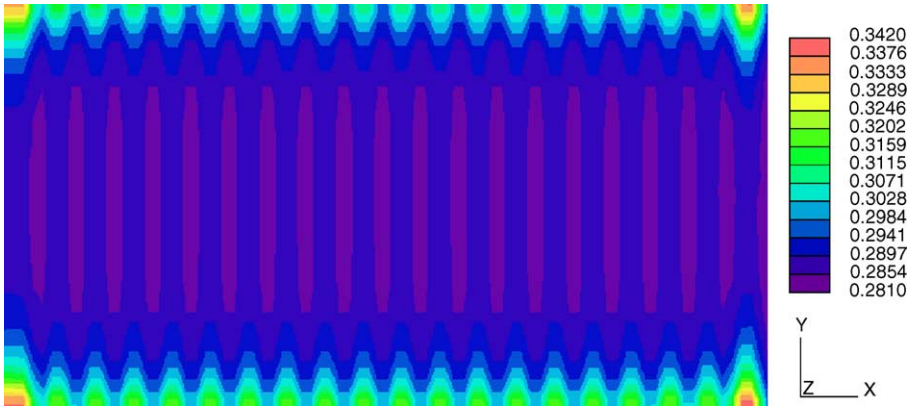

Fig. 11. Limiting current density distribution in catalyst surface (mA cm^{-2}).

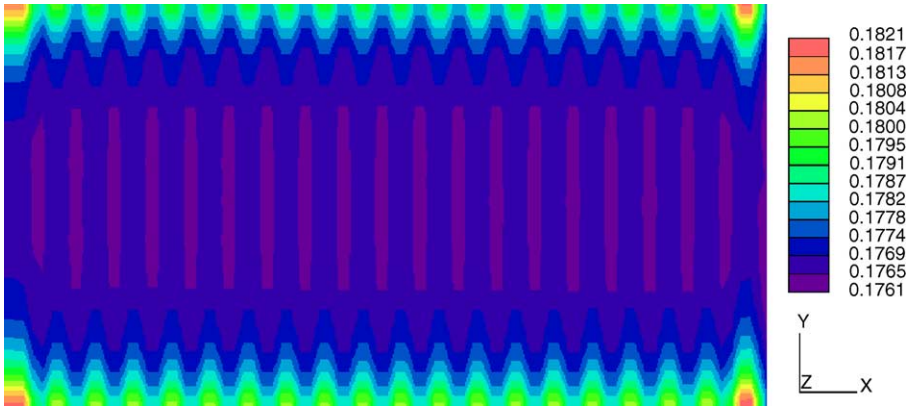

Fig. 12. Oxygen mole fraction distribution in cathode catalyst layer.

in other component which did not take into account in the numerical model. Comparing with the typical PEMFC polarization curve, it is evidential that the concentration losses of air-breathing PEMFC is much serious due to oxygen mass limitation.

Fig. 9 shows the current density distribution. Comparing with temperature distribution obtained from experiment in Fig. 7. The places where the tested temperature is high have higher current density (position 7 and 8). That means the electrochemical reaction is stronger there. These observation also proves that the numerical calculation well agree with the experiment. Fig. 10 is distribution of calculated temperature in the surface of diffusion layer that is close to cathode channel. It is almost same as the experiment results. Highest temperature is in the bottom of furthest left and right side air channel.

Fig. 11 is calculated limiting current density distribution. It can be observed that the in the regions near the air intake and vent and channels closing to anode inlet and outlet have better oxygen transportation. The lowest limiting current den-

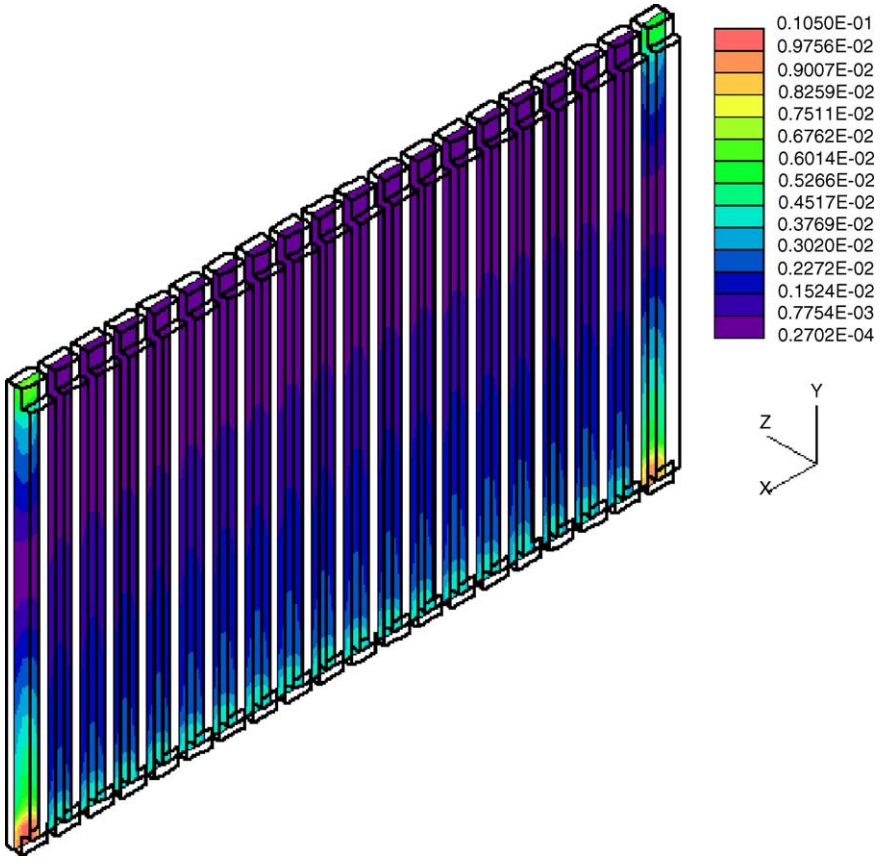

Fig. 13. Air velocity profile in cathode channel ($m\,s^{-1}$).

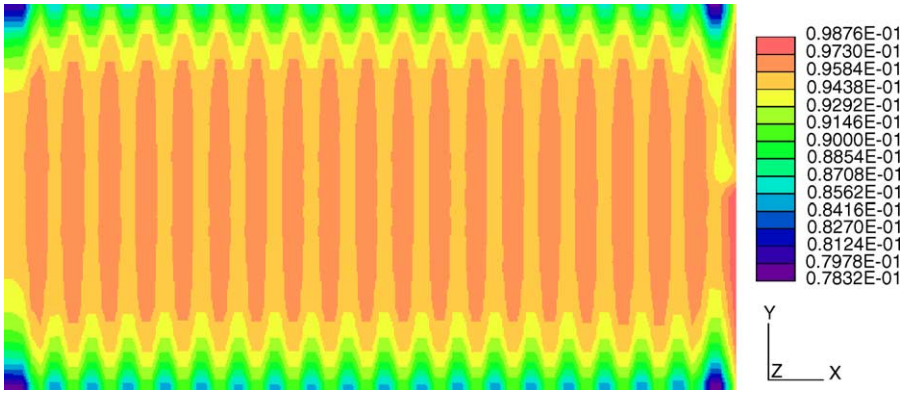

Fig. 14. Concentration losses distribution due to oxygen limitation (V).

sity is 281 mA cm^{-2}. That means the cell cannot work beyond this current density because oxygen is used up in some area. Fig. 12 is oxygen mole fraction in cathode catalyst layer. It is lower than in ambient air and channel because of consumption in electrochemical reaction and insufficient natural convection. In the side channel the oxygen mole fraction is higher due to stronger natural convection. Fig. 13 is air velocity profile in cathode channel. It can be observed some air also flow into channel from the open vent in the side channel where it is near the anode inlet and outlet. The total calculated mass flux from intake and open vent is 6.818E−7 kg s^{-1}, thus about 1.568E−7 kg s^{-1} oxygen come to catalyst layer. However, for average current density of 150 mA cm^{-2}, the oxygen usage should be 5.7E−7 kg s^{-1}, this is reason of that the PEMFC working in natural convection air supply cannot work in high current density. The distribution of concentration losses when current density load is 150 mA cm^{-2} can be found in Fig. 14. It is relatively high than typical forced convection air supply PEMFC.

5. Conclusions

A comprehensive three-dimensional computational model of an air-breathing PEMFC has been developed, with the validation by experiment. The model accounts for all major transport phenomena of fluid dynamic, heat/mass transfer, electrochemical reactions in a single air-breathing PEMFC except the phase change of water. A testing system has been designed to investigate the performance and temperature distribution of an air-breathing PEMFC. The experiments have been done under different ambient humidity. The results from numerical simulation are physical consistent and in good agreement with experiment data. The distributions of velocity, species concentration, temperature, current density, over-potential, limiting current density, etc. have been obtained from simulation. The capabilities of the model has been demonstrated for providing detailed insight into interaction of natural convection and electrochemical reaction, onset of mass transport limitation; understanding the water transport mechanism in membrane; predicting the cell performance. The model can be easily used as a design tool for air-breathing PEMFCs in the future.

References

[1] S. Ha, B. Adams, R.I. Masel, J. Power Sources 128 (2004) 119–124.
[2] J.P. Meyers, H.L. Maynard, J. Power Sources 109 (2002) 76–88.
[3] T. Hottinen, M. Mikkola, P. Lund, J. Power Sources (2004).
[4] M. Noponen, T. Mennola, M. Mikkola, T. Hottinen, P. Lund, J. Power Sources 106 (2002) 304–312.
[5] D. Chu, R. Jiang, J. Power Sources 83 (1999) 128–133.
[6] P.-W. Li, T. Zhang, Q.-M. Wang, L. Schaefer, M.K. Chyu, J. Power Sources 114 (2003) 63–69.
[7] D.M. Bernadi, M.W. Verbruge, AIChE J. 37 (8) (1991) 1151–1163.
[8] D.M. Bernadi, M.W. Verbruge, J. Electrochem. Soc. 139 (9) (1992) 2477–2491.
[9] T.E. Springer, T.A. Zawodzinski, S. Gottesfeld, J. Electrochem. Soc. 138 (8) (1991) 2334–2341.
[10] T.F. Fuller, J. Newman, J. Electrochem. Soc. 140 (5) (1993) 1218–1225.
[11] T.V. Nguyen, R.E. White, J. Electrochem. Soc. 140 (8) (1993) 2178–2186.
[12] J.S. Yi, T.V. Nguyun, J. Electrochem. Soc. 145 (4) (1998) 1149–1159.
[13] T.E. Springer, M.S. Wilson, S. Gottesfeld, J. Electrochem. Soc. 140 (12) (1993) 3513–3526.
[14] S. Dutta, S. Shimpalee, J.W. Van Zee, J. Appl. Electrochem. 30 (2000) 135–146.
[15] S. Dutta, S. Shimpalee, J.W. Van Zee, Int. J. Heat Mass Transfer 44 (2001) 2029–2042.
[16] T.-C. Jen, T. Yan, S.-H. Chan, Int. J. Heat and Mass Tranfer 46 (2003) 4157–4168.
[17] D. Natarajan, T. Van Nguyen, J. Power Source 115 (2003) 66–80.
[18] T. Berning, D.M. Lu, N. Djilali, J. Power Sources 106 (2002) 284–294.
[19] K.P. Recknagle, R.E. Williford, L.A. Chick, D.R. Reactor, M.A. Khaleel, J. Power Sources 113 (2003) 109–114.
[20] A. Schmitz, C. Ziegler, J.O. Schumacher, 2nd European PEFC Forum, Proceedings, vol. 1, pp. 297–310.
[21] P.-W. Li, L. Schaefer, Q.-M. Wang, T. Zhang, M.K. Chyu, J. Power Sources 115 (2003) 90–100.
[22] G. Prentice, Electrochemical Engineering Principles, Prentice-Hall Inc., 1991.
[23] S. Um, C.Y. Wang, K.S. Chen, Electrochem. J. Soc. 147 (2000) 4485–4493.
[24] Z.H. Wang, C.Y. Wang, K.S. Chen, J. Power Sources 94 (2001) 40–50.